**NANO EXPRESS**                                                        **Open Access**

# Photovoltaic Performance of a Nanowire/Quantum Dot Hybrid Nanostructure Array Solar Cell

Yao Wu, Xin Yan, Xia Zhang[*] and Xiaomin Ren

**Abstract**

An innovative solar cell based on a nanowire/quantum dot hybrid nanostructure array is designed and analyzed. By growing multilayer InAs quantum dots on the sidewalls of GaAs nanowires, not only the absorption spectrum of GaAs nanowires is extended by quantum dots but also the light absorption of quantum dots is dramatically enhanced due to the light-trapping effect of the nanowire array. By incorporating five layers of InAs quantum dots into a 500-nm high-GaAs nanowire array, the power conversion efficiency enhancement induced by the quantum dots is six times higher than the power conversion efficiency enhancement in thin-film solar cells which contain the same amount of quantum dots, indicating that the nanowire array structure can benefit the photovoltaic performance of quantum dot solar cells.

**Keywords:** Nanowire array, Quantum dot, Photovoltaic, Nanophotonics and photonic crystals

## Background

The incorporation of quantum dots (QDs) into solar cells has been proposed as a promising way to enhance the device conversion efficiency [1, 2]. Insertion of QDs into the active region of a solar cell allows one to engineer the effective bandgap of the material and extend the absorption spectrum [3–6]. This can be used to enhance the photocurrent of a homogeneous solar cell [7–9] or to form an isolated intermediate band within the bandgap of the host material to absorb photons with energy below host material energy gap [10–13]. However, to surpass the efficiency of conventional devices, the absorption enhancement caused by QDs must be improved significantly. This may be achieved by increasing the number of QDs, by enhancing the optical absorption, or a combination of both [14]. In recent years, an attractive structure has been fabricated by growing Stranski-Krastanov (S-K) QDs on the sidewalls of nanowires (NWs), which offers an innovative approach to combine the advantage of the two kinds of nanostructures [15–19]. Multilayer QDs can be grown on the sidewalls of NWs, which substantially increase the number of QDs, while the

vertically aligned NW array can dramatically enhance the absorption of QDs due to the excellent light-trapping ability [20–24]. Thus, the photocurrent contributed by QDs in the NW/QD hybrid nanostructure array is expected to be larger than that in thin-film QD structures. Moreover, the NW/QD hybrid structure can be fabricated on low-cost silicon substrates, which makes it promising for low-cost, high-efficiency solar cells [25]. Although the fabrication and optical properties of NW/QD hybrid nanostructures have been widely reported, the performance of solar cells based on the hybrid structures has not been investigated yet.

In this paper, a coupled optoelectronic simulation is presented to investigate the photovoltaic performance of a GaAs/InAs NW/QD hybrid solar cell. The considered structure consists of a vertically aligned NW array with each NW containing five layers of QDs arranged perpendicular to the NW growth axis. Both the QDs and the wetting layers (WLs) contribute to sub-bandgap photon absorption, extending the absorption spectrum to 950 nm. Each NW consists of a radial pin junction with all of the QD layers located in the intrinsic region. At first, a comparison in light absorption spectra between the NW arrays with and without QDs is made by using three-dimensional finite-difference time-domain (3D-FDTD)

* Correspondence: xzhang@bupt.edu.cn
State Key Laboratory of Information Photonics and Optical Communications, Beijing University of Posts and Telecommunications, Beijing 100876, China

Wu *et al. Nanoscale Research Letters* (2018) 13:62

Page 2 of 7

simulations. The absorption spectra of their thin-film counterparts are calculated as well. Then, the photogeneration profiles are incorporated into the electrical simulations to calculate the current density versus voltage (*I-V*) characteristics. The results show that, in both NW array and thin-film solar cells, incorporation of QDs can enhance the short-circuit current ($J_{sc}$) by increasing light absorption; however, a degeneration of open-circuit voltage ($V_{oc}$) occurs at the same time. The overall power conversion efficiency enhancement induced by the quantum dots in NW array solar cells is six times higher than the efficiency enhancement in thin-film solar cells which contain the same amount of quantum dots, indicating that the NW array structure can benefit the photovoltaic performance of quantum dot solar cells.

## Methods

In our previous study [15], the fabrication of the NW/QD hybrid structures was realized by using a Thomas Swan Close Coupled Showerhead (CCS) metal organic chemical vapor deposition (MOCVD) system. Trimethylgallium (TMGa), trimethylindium (TMIn), and arsine (AsH₃) were used as precursors. The carrier was hydrogen. An Au-coated GaAs substrate was loaded into the MOCVD reactor and annealed under AsH₃ ambient to form Au-Ga alloy particles as catalyst. The GaAs NWs were grown in the first place, and then the first shell of InAs QDs was deposited by switching off TMGa and raising the temperature. After the growth of the InAs QD layer, the GaAs spacer shell was radially grown on the InAs QDs.
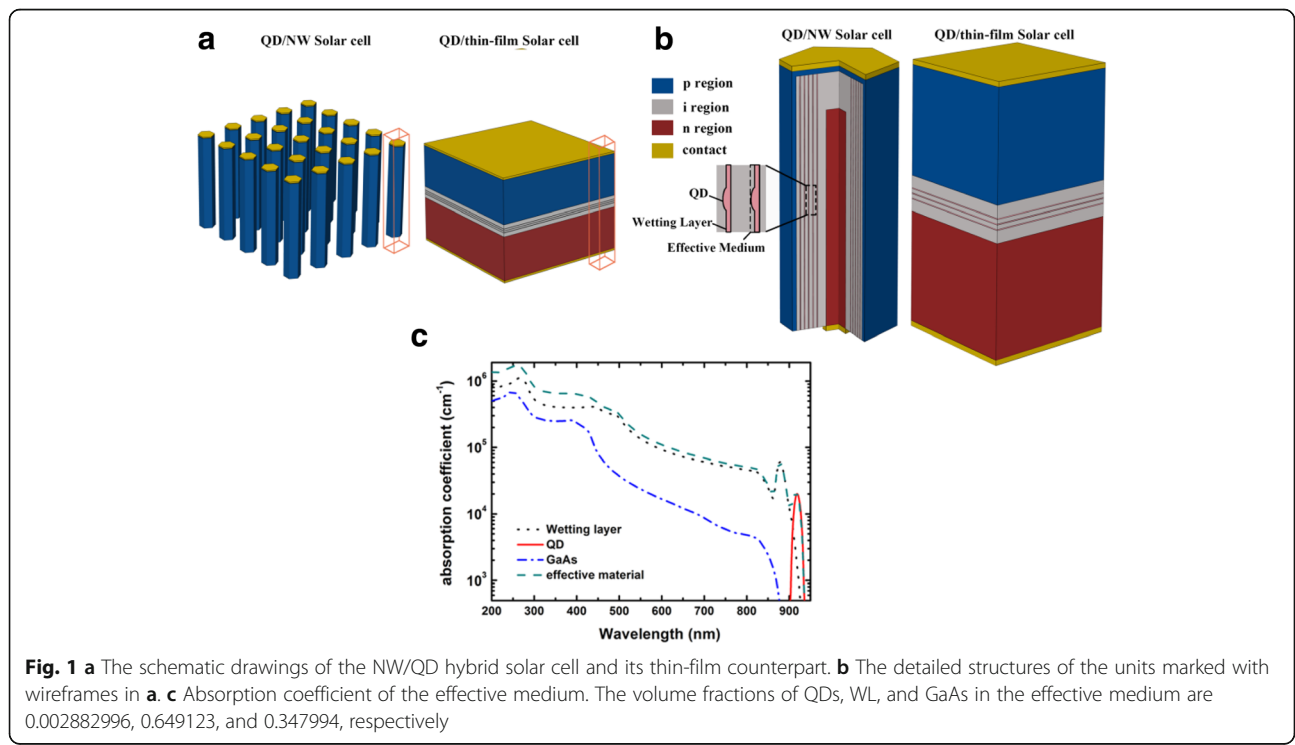
The multilayers of QD structures were realized by repeating the combination of InAs QDs and GaAs spacer shell for certain times.
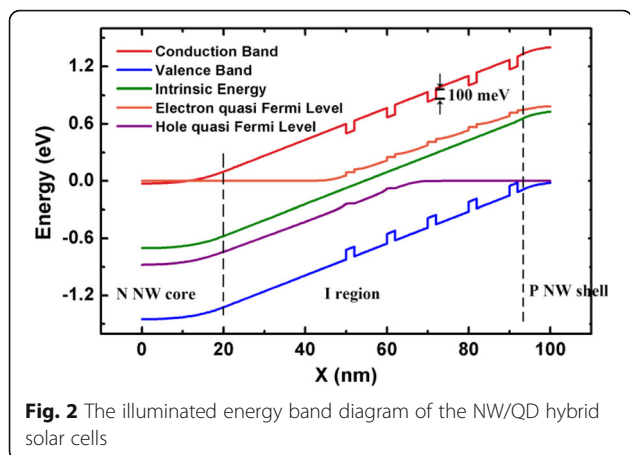
The schematic of the NW/QD hybrid solar cell is illustrated in Fig. 1a. The device consists of periodic GaAs/InAs NW/QD hybrid structures. Each NW contains a radial pin junction with five layers of QDs arranged perpendicular to the NW growth axis in the intrinsic region, as shown in Fig. 1b. The doping concentration of the p-type shell and n-type core is $3 \times 10^{18}$ and $1 \times 10^{18}$ cm$^{-3}$, respectively. The QD layers are modeled by treating InAs QDs, WL, and GaAs material surrounding QDs as an effective medium. The thickness of each effective medium is 2 nm.

For optical simulation, the wavelength-dependent complex refractive index of the effective medium is calculated by a volume-weighted superposition of the QDs, WL, and GaAs material as described in [26], which is expressed by Eq. (1).

$$\alpha_{eff} = F_{QD}\alpha_{QD} + F_{WL}\alpha_{WL} + F_{GaAs}\alpha_{GaAs} \qquad (1)$$

where $F_{QD}$, $F_{WL}$, and $F_{GaAs}$ are the volume fractions of QD, WL, and GaAs materials in the effective medium, respectively. The absorption coefficient of InAs QDs and WLs is obtained from [26], with the same QD size and density. Other material parameters are obtained from [27]. The absorption coefficient used in this work is presented in Fig. 1c. Two peaks are observed below GaAs bandgap, with one centered at a wavelength of 876 nm



**Fig. 1 a** The schematic drawings of the NW/QD hybrid solar cell and its thin-film counterpart. **b** The detailed structures of the units marked with wireframes in **a**. **c** Absorption coefficient of the effective medium. The volume fractions of QDs, WL, and GaAs in the effective medium are 0.002882996, 0.649123, and 0.347994, respectively

Wu *et al. Nanoscale Research Letters* (2018) 13:62

Page 3 of 7



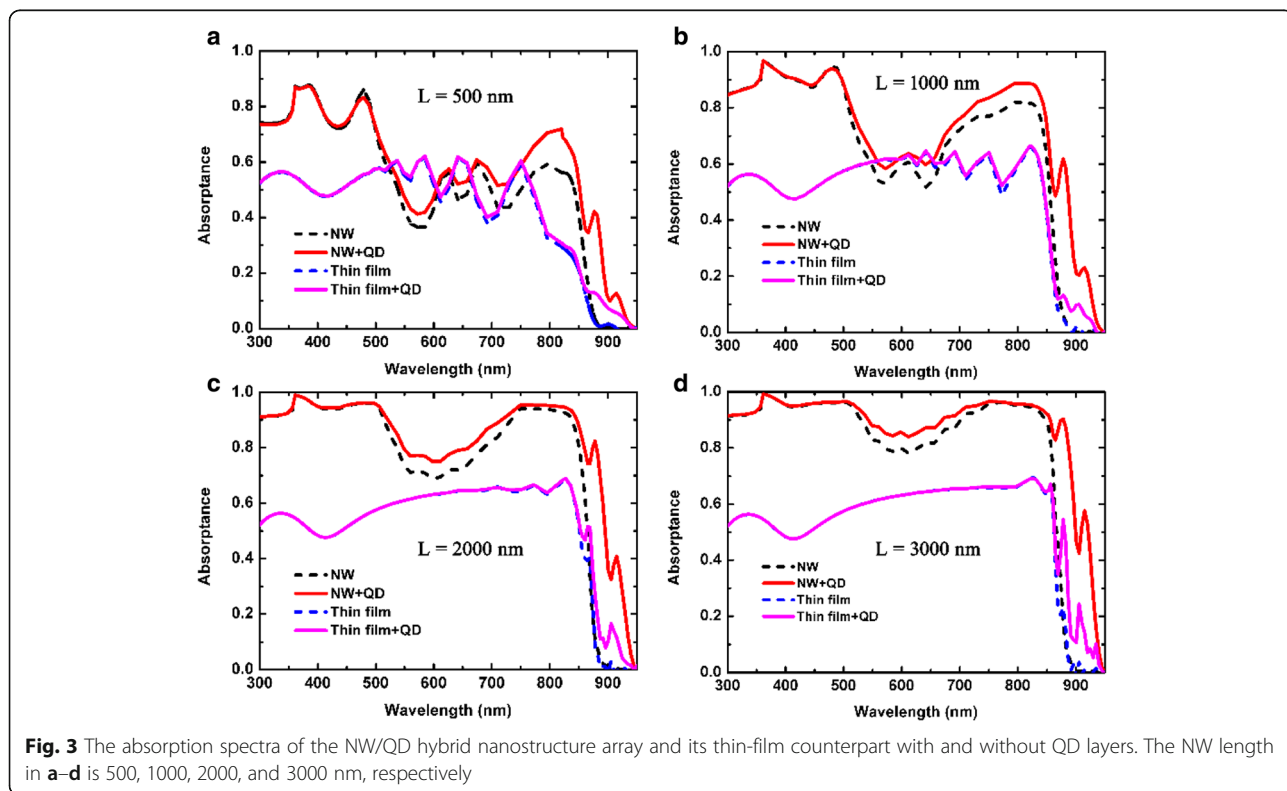**Fig. 2** The illuminated energy band diagram of the NW/QD hybrid solar cells

and the other centered at 916 nm, which are attributed to the QD layers. The thin-film solar cell containing QD layers is also simulated for comparison. Thickness of the thin-film solar cell is set to be equal to the NW length, and the total volume of QD layers and the thickness of the intrinsic layer in the thin-film solar cells are set to be the same with those in the NW/QD hybrid solar cells. The absorption properties of the solar cells are calculated by the FDTD Solutions software package (Lumerical Solutions, Inc.). By placing periodic boundary conditions, the simulations can be carried out in a single unit cell to model the periodic array structure. The AM1.5G spectrum is divided

into 87 discrete wavelength intervals, from 300 to 950 nm. The transverse electric (TE) and transverse magnetic (TM) mode contributions are superimposed to model the corresponding unpolarized feature of sunlight. The total optical generation under AM1.5G illumination can be modeled by superimposing the spectrally resolved single-wavelength photogeneration rates.

For electrical modeling, the 3D optical generation profiles are incorporated into the finite-element mesh of the devices in the Device software package (Lumerical Solutions, Inc.), which solves the carrier continuity equations coupled with Poisson's equation self-consistently. To model the carrier transport properties of the effective medium, we assume that the optical generated carriers in GaAs barriers are captured by the lower bandgap 2D WL and, subsequently, relax to the QD ground state on time scales of 1–50 ps [28, 29]. The carriers generated in QDs or captured from WL recombine or escape back to WL through thermal emission [30]. The capture and escape process is modeled by setting 100 meV effective band offsets at the interface of GaAs and effective medium, according to the activation energy for thermal emission from quantum dots reported in literatures [30–32]. A similar modeling method has been reported in [26], in which the characteristics of QD-enhanced multijunction solar cells have been investigated. The illuminated energy band diagram of the NW/QD hybrid solar cells is shown in Fig. 2.



**Fig. 3** The absorption spectra of the NW/QD hybrid nanostructure array and its thin-film counterpart with and without QD layers. The NW length in **a**–**d** is 500, 1000, 2000, and 3000 nm, respectively

Wu *et al. Nanoscale Research Letters* (2018) 13:62

Page 4 of 7

Radiative, Auger, and Shockley-Read-Hall (SRH) recombination is taken into consideration in the device electrical simulation. The QD minority carrier lifetimes are described using a radiative recombination lifetime of 1 ns and a SRH recombination lifetime of 10 ns [26], the final lifetimes of the effective medium are a weighted sum of the QD and GaAs NW recombination lifetimes (assuming carriers captured by the WL are subsequently captured by the QD), as described in [26]. The Auger recombination coefficient of the effective medium is set to $4.2 \times 10^{-29}$ cm$^6$/s [33]. And, the electron and hole effective masses are set to $0.053m_0$ and $0.341m_0$, respectively [26]. In modeling of the transport of barrier carriers across the effective medium region, we use the barrier mobility (2500 cm$^2$/Vs for electrons and 150 cm$^2$/Vs for holes) [34], as described in [35]. A surface recombination velocity of 3000 cm/s is used in the device model, assuming the nanowire surfaces are well passivated [34, 36]. And, the contact minority carrier recombination velocity is set to be $10^7$ cm/s [37].

## Results and Discussion

The absorption spectra of GaAs NW array solar cells with and without QD layers are shown in Fig. 3. The NW radius is set to 100 nm, and the period is 360 nm.

By introducing QD layers, the absorption of GaAs NWs is dramatically enhanced and the absorption spectrum is extended to 950 nm. Figure 3a–d shows the absorption spectra with different NW lengths. It can be seen that the absorption is markedly increased by QD layers at a wavelength beyond 450 nm, since the QD layers have higher absorption coefficient than GaAs NWs. As the NW length increases, the absorption difference between NW arrays with and without QD layers is getting smaller in the wavelength range beyond the GaAs bandgap, indicating that the absorption of GaAs is more sufficient for longer NWs. While in the wavelength range below the GaAs bandgap, as GaAs NWs contribute little to light absorption, the absorption enhancement induced by QD layers becomes more prominent as the NW length increases. Two absorption peaks are observed in the wavelength range below the GaAs bandgap, which are centered at 876 and 916 nm, respectively, corresponding to the wavelengths at which the effective medium has the highest absorption coefficient. Compared with the NW/QD hybrid solar cell, the absorption of the thin-film solar cell saturates much earlier with the increase of film thickness, as the main loss in the thin-film solar cell is reflection. As the volume ratio of QD layers in the
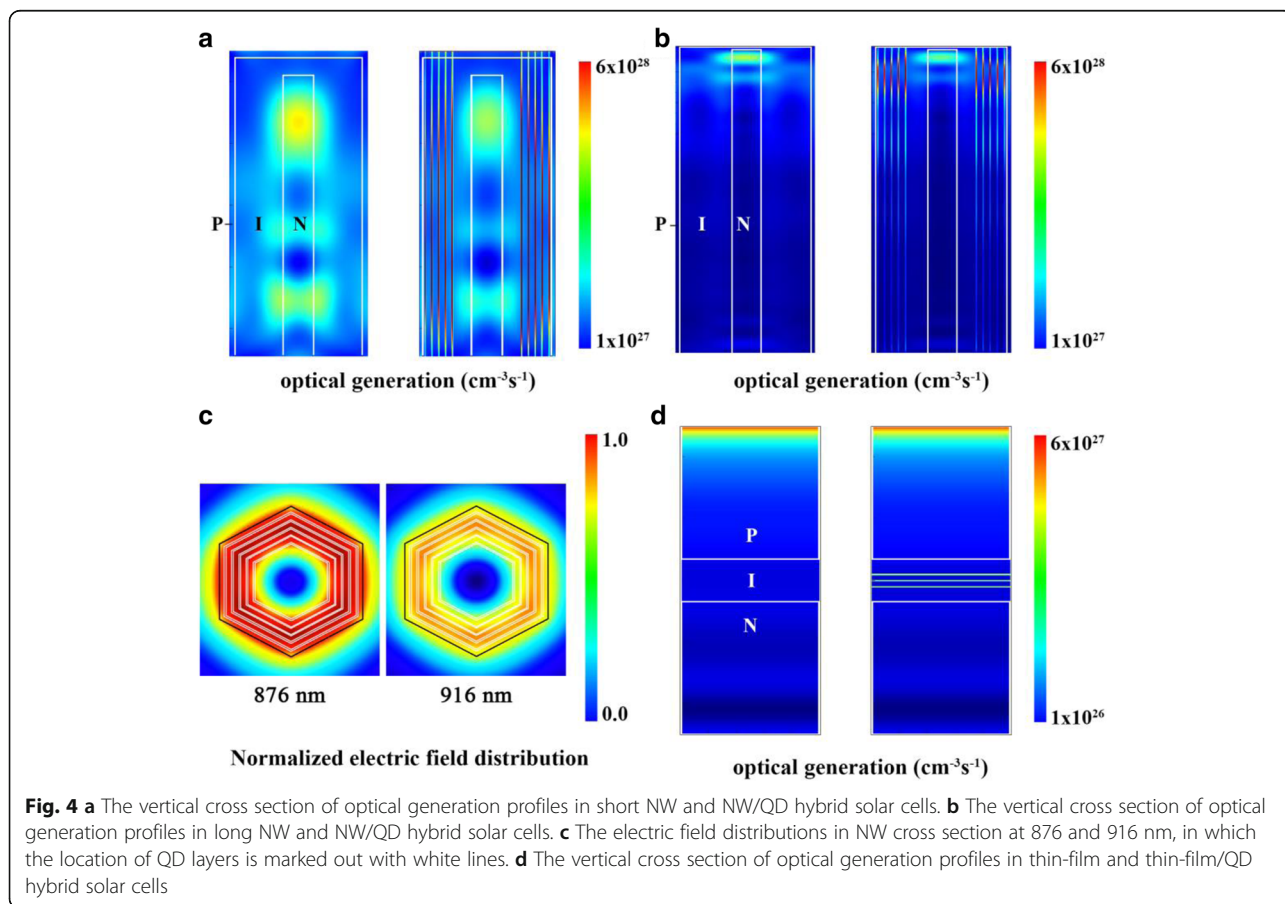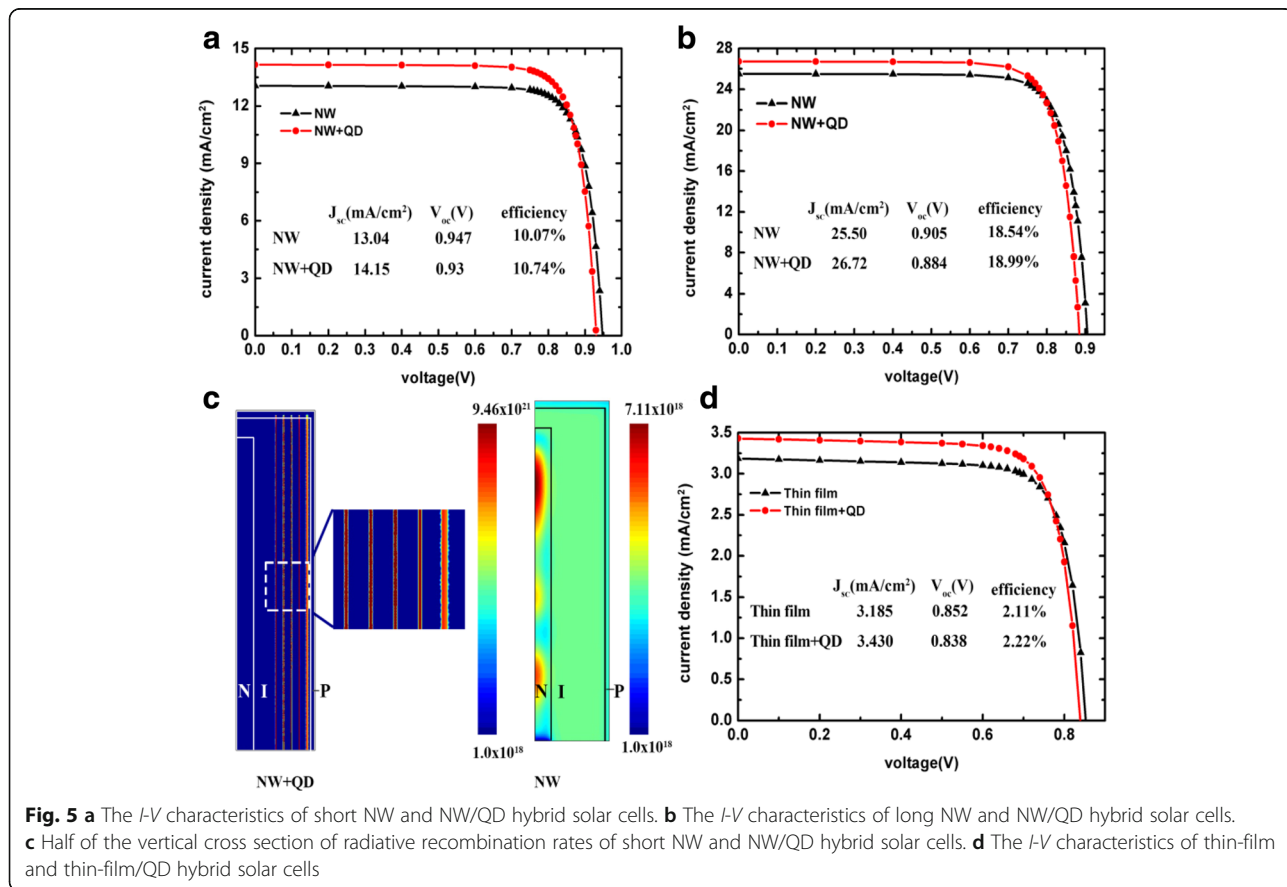


**Fig. 4 a** The vertical cross section of optical generation profiles in short NW and NW/QD hybrid solar cells. **b** The vertical cross section of optical generation profiles in long NW and NW/QD hybrid solar cells. **c** The electric field distributions in NW cross section at 876 and 916 nm, in which the location of QD layers is marked out with white lines. **d** The vertical cross section of optical generation profiles in thin-film and thin-film/QD hybrid solar cells

Wu *et al. Nanoscale Research Letters* (2018) 13:62

Page 5 of 7

thin films is much lower than that in the NW array, the light absorption enhancement induced by QD layers is almost negligible in the wavelength range beyond the GaAs bandgap. While in the wavelength range below the GaAs bandgap, due to the lack of light-trapping ability, the absorption of QD layers in the thin film is much lower than that in the NW array.

The optical generation profiles of the considered structures are shown in Fig. 4. NWs with lengths of 500 and 3000 nm are considered in this part (hereafter referred to as the short NW and the long NW, respectively). It is obvious that the carrier generation in effective medium is much higher than that in GaAs, demonstrating the absorption enhancement induced by QDs. In NW/QD hybrid solar cells, fewer carriers are generated in the NW core region, since some carriers are concentrated in QD regions instead. This phenomenon is expected to benefit the device performance, as the highly doped core region often suffers from serious recombination loss. In short NWs, the optical generated carriers distribute in the whole NW, while in long NWs, carriers are mainly concentrated at the top, indicating that the light absorption in long NWs is sufficient although the considered NW array does not contain any substrates. It can be observed that, in long NWs, a high carrier generation

region in QD layers stretches longer than that in the NW core, and the carriers are concentrated to several lobes along the NW axis. This is induced by the resonance modes at a long-wavelength region in the NW. Long wavelength light has longer absorption length and is mainly absorbed in QD regions, especially the light at a wavelength range below GaAs bandgap. The electric field distributions under unpolarized light illumination in GaAs NWs at 876 and 916 nm are shown in Fig. 4c, from which we can see that the electric field strongly overlaps with the QD regions, which further explains the enhancing effect of NW structures on the QD absorption at this wavelength. The optical generation profile of a 500-nm thin-film solar cell is shown in Fig. 4d, and it can be seen that the absorption in thin-film structures is much weaker than that in NWs. For thin-film structures, the carriers generated in QDs have little effect on the overall generation profile. While in NWs, QDs with the same volume can contribute to absorption significantly thanks to guided-resonance modes in NWs [21].

Further studies focus on investigation of the potential increase in photovoltaic efficiency gains stemming from the absorption enhancement induced by QDs. Previously simulated photogeneration profiles are incorporated into the Device software package to calculate the *I-V* characteristics



**Fig. 5 a** The *I-V* characteristics of short NW and NW/QD hybrid solar cells. **b** The *I-V* characteristics of long NW and NW/QD hybrid solar cells. **c** Half of the vertical cross section of radiative recombination rates of short NW and NW/QD hybrid solar cells. **d** The *I-V* characteristics of thin-film and thin-film/QD hybrid solar cells

Wu et al. Nanoscale Research Letters (2018) 13:62

Page 6 of 7

of considered devices. Carrier generation is expected to be increased in QD regions; however, carriers in QD regions suffer from higher recombination rate. As a result, an enhancement of short-circuit currents ($J_{sc}$) in QD-enhanced solar cells is often accompanied by a deterioration of open-circuit voltage ($V_{oc}$) [38]. The effect of QDs on device efficiency depends on a trade-off between $J_{sc}$ increase and $V_{oc}$ reduction. The I-V characteristics of the NW solar cells are shown in Fig. 5a, b, and corporation of QDs in short NWs leads to a $J_{sc}$ enhancement of 1.09 mA/cm$^2$ and a $V_{oc}$ reduction of 0.017 V. While in long NWs, a $J_{sc}$ increase of 1.22 mA/cm$^2$ and a $V_{oc}$ reduction of 0.021 V are observed. The overall efficiency increase is 0.67% in short NWs and 0.45% in long NWs. By increasing the NW length, the $J_{sc}$ enhancement is increased as well as the $V_{oc}$ reduction due to the increase of QD volume. Figure 5c illustrates the radiative recombination profiles in NWs near $V_{oc}$; compared with pure GaAs NWs, the radiative recombination rates increase by more than 3 orders of magnitude in the QD layers, which explains the $V_{oc}$ degeneration. The conversion efficiencies of thin-film solar cells with and without QDs are calculated as well. The efficiency enhancement induced by QDs is only 0.11%, much lower than that in NWs solar cells, although the QD volumes in NWs and thin-film structures are the same. The result indicates that NW array is advantageous to enhancing efficiency of quantum dot solar cells. The efficiency enhancement induced by QDs is not so impressive in this work due to the degeneration of $V_{oc}$; however, several approaches have been demonstrated to maintain $V_{oc}$ in QD-enhanced solar cells [5, 39]. More satisfying efficiency enhancement is expected to be obtained if the $V_{oc}$ degeneration could be avoided in NW/QD hybrid solar cells. Moreover, the optical absorption spectrum of QDs depends strongly on the dot size distribution [40, 41, 42]. We believe that, by modifying the QD size and density, it is possible to achieve higher absorption coefficient, which may lead to more significant absorption enhancement and higher conversion efficiency.

## Conclusions

In summary, we have studied the photovoltaic performance of a GaAs/InAs NW/QD hybrid solar cell. The results show that the absorption spectra of GaAs NWs can be extended to 950 nm by incorporating multilayer InAs QDs on the NW sidewalls. The absorption of QDs is also dramatically improved due to the light-trapping effect of the NW array. I-V characteristics show that $J_{sc}$ in NW solar cells can be increased due to light absorption enhancement, while $V_{oc}$ is degenerated because of more serious recombination induced by QDs. The overall efficiency enhancement induced by QDs in NW solar cells is much higher than that in thin-film solar cells,

indicating that the GaAs/InAs NW/QD hybrid structure is promising for QD solar cells.

## Authors' Contributions
YW, XY, XZ, and XR performed the simulations and analyzed the results. YW, XY, and XZ conceived and designed the structure and simulations and participated in writing the manuscript. All authors read and approved the final manuscript.

## Authors' Information
YW (Ph.D.), XY (Ph.D.), XZ (professor), and XR (professor) are from the State Key Laboratory of Information Photonics and Optical Communications, Beijing University of Posts and Telecommunications, Beijing 100876, China.

## Publisher's Note
Springer Nature remains neutral with regard to jurisdictional claims in published maps and institutional affiliations.

## References
1. Wu J, Yu P, Susha AS, Sablon KA, Chen H, Zhou Z, Li H, Ji H, Niu X, Govorov AO, Rogach AL, Wang ZM (2015) Broadband efficiency enhancement in quantum dot solar cells coupled with multispiked plasmonic nanostars. Nano Energy 13:827–835
2. Zheng Z, Ji H, Yu P, Wang Z (2016) Recent progress towards quantum dot solar cells with enhanced optical absorption. Nanoscale Res Lett 11(1):266
3. Driscoll K, Bennett MF, Polly SJ, Forbes DV, Hubbard SM (2014) Effect of quantum dot position and background doping on the performance of quantum dot enhanced GaAs solar cells. Appl Phys Lett 104(2):023119
4. Guimard D, Morihara R, Bordel D, Tanabe K, Wakayama Y, Nishioka M, Arakawa Y (2010) Fabrication of InAs/GaAs quantum dot solar cells with enhanced photocurrent and without degradation of open circuit voltage. Appl Phys Lett 96(20):203507
5. Bailey CG, Forbes DV, Raffaelle RP, Hubbard SM (2011) Near 1 V open circuit voltage InAs/GaAs quantum dot solar cells. Appl Phys Lett 98(16):163105
6. Lin C, Liu W, Shih C (2011) Detailed balance model for intermediate band solar cells with photon conservation. Opt Express 19(18):16927–16933
7. Lee Y, Yao Y, Tsai M, Liu A, Yang M, Lai J (2013) Current matching using CdSe quantum dots to enhance the power conversion efficiency of InGaP/GaAs/Ge tandem solar cells. Opt Express 21(26):A953–A963
8. Kerestes C, Polly S, Forbes D, Bailey C, Podell A, Spann J, Patel P, Richards B, Sharps P, Hubbard S (2014) Fabrication and analysis of multijunction solar

Wu *et al. Nanoscale Research Letters* (2018) 13:62

Page 7 of 7

cells with a quantum dot (In) GaAs junction. Prog Photovolt Res Appl 22(11):1172–1179

9. Walker AW, Theriault O, Hinzer K (2014) The dependence of multijunction solar cell performance on the number of quantum dot layers. IEEE J Quantum Electron 50(3):198–203

10. Tomić S, Jones STS, Harrison NM (2008) Absorption characteristics of a quantum dot array induced intermediate band: implications for solar cell design. Appl Phys Lett 93(26):263105

11. Luque A, Martí A (1997) Increasing the efficiency of ideal solar cells by photon induced transitions at intermediate levels. Phys Rev Lett 78(26):5014

12. Bailey CG, Forbes DV, Polly SJ, Bittner ZS, Dai Y, Mackos C, Raffaelle RP, Hubbard SM (2012) Open-circuit voltage improvement of InAs/GaAs quantum-dot solar cells using reduced InAs coverage. IEEE J Photovoltaics 2(3):269–275

13. Yu P, Wu J, Gao L, Liu H, Wang Z (2017) InGaAs and GaAs quantum dot solar cells grown by droplet epitaxy. Sol Energ Mat Sol C 161:377–381

14. Mellor A, Luque A, Tobías I, Martí A (2014) The feasibility of high-efficiency InAs/GaAs quantum dot intermediate band solar cells. Sol Energ Mat Sol Cells 130:225–233

15. Yan X, Zhang X, Li J, Cui J, Ren X (2015) Fabrication and optical properties of multishell InAs quantum dots on GaAs nanowires. J Appl Phys 117(5):054301

16. Uccelli E, Arbiol J, Morante JR, Fontcuberta i Morral A (2010) InAs quantum dot arrays decorating the facets of GaAs nanowires. ACS Nano 4(10):5985–5993

17. Yan X, Zhang Z, Ren X, Lv X, Li J, Wang Q, Cai S, Huang Y (2012) Formation mechanism and optical properties of InAs quantum dots on the surface of GaAs nanowires. Nano Lett 12(4):1851–1856

18. Yan X, Zhang X, Ren X, Li J, Lv X, Wang Q, Huang Y (2012) Growth and photoluminescence of InxGa1−xAs quantum dots on the surface of GaAs nanowires by metal organic chemical vapor deposition. Appl Phys Lett 101(2):023106

19. Yan X, Zhang X, Ren X, Huang H, Guo J, Guo X, Liu M, Wang Q, Cai S, Huang Y (2011) Growth of InAs quantum dots on GaAs nanowires by metal organic chemical vapor deposition. Nano Lett 11(9):3941–3945

20. Jung J, Guo Z, Jee S, Um H, Park K, Lee J (2010) A strong antireflective solar cell prepared by tapering silicon nanowires. Opt Express 18(103):A286–A292

21. Wen L, Zhao Z, Li X, Shen Y, Guo H, Wang Y (2011) Theoretical analysis and modeling of light trapping in high efficiency GaAs nanowire array solar cells. Appl Phys Lett 99(14):143116

22. Huang N, Lin C, Povinelli ML (2012) Broadband absorption of semiconductor nanowire arrays for photovoltaic applications. J Opt 14(2):024004

23. Garnett E, Yang P (2010) Light trapping in silicon nanowire solar cells. Nano Lett 10(3):1082–1087

24. Yu P, Wu J, Liu S, Xiong J, Jagadish C, Wang ZM (2016) Design and fabrication of silicon nanowires towards efficient solar cells. Nano Today 11(6):704–737

25. Yan X, Zhang X, Li J, Cui J, Wang Q, Huang Y, Ren X (2013) Growth of InAs quantum dots on Si-based GaAs nanowires by controlling the surface adatom diffusion. J Cryst Growth 384:82–87

26. Walker AW, Thériault O, Wheeldon JF, Hinzer K (2013) The effects of absorption and recombination on quantum dot multijunction solar cell efficiency. IEEE J Photovolt 3(3):1118–1124

27. Palik ED (1985) Handbook of optical constants of solids-I. Academic, USA

28. Ferreira R, Bastard G (1999) Phonon-assisted capture and intradot Auger relaxation in quantum dots. Appl Phys Lett 74(19):2818

29. Narvaez GA, Bester G, Zunger A (2006) Carrier relaxation mechanisms in self-assembled (In,Ga)As/GaAs quantum dots: efficient P→S Auger relaxation of electrons. Phys Rev B 74(7):075403

30. Yang W, Lowe-Webb RR, Lee H, Sercel PC (1997) Effect of carrier emission and retrapping on luminescence time decays in InAs/GaAs quantum dots. Phys Rev B 56(20):13314

31. Brusaferri L, Sanguinetti S, Grilli E, Guzzi M, Bignazzi A, Bogani F, Carraresi L, Colocci M, Bosacchi A, Frigeri P, Franchi S (1996) Thermally activated carrier transfer and luminescence line shape in self-organized InAs quantum dots. Appl Phys Lett 69(22):3354

32. Fafard S, Raymond S, Wang G, Leon R, Leonard D, Charbonneau S, Merz JL, Petroff PM, Bowers JE (1996) Temperature effects on the radiative recombination in self-assembled quantum dots. Surf Sci 361:778–782

33. Bhattacharya P, Ghosh S, Pradhan S, Singh J, Wu Z, Urayama J, Kim K, Norris TB (2003) Carrier dynamics and high-speed modulation properties of tunnel injection InGaAs-GaAs quantum-dot lasers. IEEE J Quantum Electron 39(8):952–962

34. Huang N, Lin C, Povinelli ML (2012) Limiting efficiencies of tandem solar cells consisting of III-V nanowire arrays on silicon. J Appl Phys 112(6):064321

35. Ramey SM, Khoie R (2003) Modeling of multiple-quantum-well solar cells including capture, escape, and recombination of photoexcited carriers in quantum wells. IEEE T Electron Dev 50(5):1179–1188

36. Joyce HJ, Docherty CJ, Gao Q, Tan HH, Jagadish C, Lloyd-Hughes J, Herz LM, Johnston MB (2013) Electronic properties of GaAs, InAs and InP nanowires studied by terahertz spectroscopy. Nanotechnology 24(21):214006

37. Wang X, Khan MR, Lundstrom M, Bermel P (2014) Performance-limiting factors for GaAs-based single nanowire photovoltaics. Opt Express 22(S2):A334–A358

38. Jolley G, Lu HF, Fu L, Tan HH, Jagadish C (2010) Electron-hole recombination properties of In0.5Ga0.5As/GaAsIn0.5Ga0.5As/GaAs quantum dot solar cells and the influence on the open circuit voltage. Appl Phys Lett 97(12):123505

39. Lam P, Hatch S, Wu J, Tang M, Dorogan VG, Mazur YI, Salamo GJ, Ramiro I, Seeds A, Liu H (2014) Voltage recovery in charged InAs/GaAs quantum dot solar cells. Nano Energy 6:159–166

40. Ferreira DL, Alves JLA (2004) The effects of shape and size nonuniformity on the absorption spectrum of semiconductor quantum dots. Nanotechnology 15(8):975

41. Tomić S, Sogabe T, Okada Y (2015) In-plane coupling effect on absorption coefficients of InAs/GaAs quantum dots arrays for intermediate band solar cell. Prog Photovolt Res Appl 23(5):546–558

42. Mellor A, Luque A, Tobías I, Martí A (2013) A numerical study into the influence of quantum dot size on the sub-bandgap interband photocurrent in intermediate band solar cells. AIP Adv 3(2):022116